Bilge International Journal of Science and Technology Research
ISSN: 2651-401X
e-ISSN: 2651-4028
Research Article
2023, Volume: 7, Issue: 1, 70-77
Received: 09.11.2022; Accepted: 14.02.2023
DOI: 10.30516/bilgesci.1201697

Simulation of Load Behavior Based on Perturb-Observation Method in Non-Isolated Boost Converter for Maximum Power Point Tracking of Thermoelectric Generators

Hayati Mamur[1*], Çiğdem Akyıldız[1], Mehmet Ali Üstüner[1]

Abstract: The efficiency of thermoelectric generators (TEGs) is quite low. To operate the TEGs at the maximum power point (MPP), the internal resistance of the connected load and the TEG must be equal. This is not always possible. For this, converters containing the maximum power point tracking (MPPT) algorithm tracking MPP are placed between the TEG and the load. These converters cannot perform MPPT on every connected load value. The aim of this study is to investigate and highlight at which load values MPPT can be performed in non-isolated boost converters by using perturb & observation (P&O) method. For this purpose, a 50 W converter was designed with a 45.76 W TEG in MATLAB/Simulink environment. Load resistances have been increased starting from the minimum value up to 5.84 ohm being the internal resistance value of the TEG. For this case, the amount of error in MPPT was large up to the internal resistance value of the TEG. In other words, the P&O algorithm could not perform MPPT. When the load resistance value started from 5.84 ohms and increased to larger values, MPPT could be performed by means of the non-isolated boost converter with the P&O algorithm.

Keywords: Thermoelectric generator, MPPT, Boost converter, Load limit.

[1]**Address:** Manisa Celal Bayar University, Manisa/Türkiye

***Corresponding author**: hayati.mamur@cbu.edu.tr

Citation: Mamur, H., Akyıldız, Ç., Üstüner, M.A. (2023). Simulation of Load Behavior Based on Perturb-Observation Method in Non-Isolated Boost Converter for Maximum Power Point Tracking of Thermoelectric Generators. Bilge International Journal of Science and Technology Research, 7(1): 70-77.

1. INTRODUCTION

Thermoelectric generators (TEG) used to recover waste heat are semiconductor elements. Their output power raises in direct proportion to the temperature difference between their surfaces (Mamur et al., 2021). Since the efficiency of TEGs is low, it is important to generate maximum power for improving their working performance and ensure that they work close to full capacity (Mamur and Ahiska, 2015). To generate maximum power from the TEG, the overall internal resistance of the TEG setup and the external load resistance linked to the TEG must be equal (Bond et al., 2015). Ahmet et al. (2022) used a load resistor and a boost converter under different conditions to compare MPPT algorithms in photovoltaic (PV) systems. In the load resistance calculation and converter design, they did not specify the exact value of the resistance value in the PV system model. Dileep and Singh (2017) focused on the connection between converters and load resistors. They explained the relationship between the load resistors and the input impedance according to the converter type in their study. Attar et al. (2020) conducted a study to find the optimum electrical load resistance in TEG systems without converters with MPPT. Khan et al. (2022) developed different algorithms for MPPT tracking by using PV and TEG systems together and used boost converter in their systems. Zafar et al. (2022) developed an algorithm using machine learning for MPPT in TEG system and used a boot converter here. They did not mention which loads can be connected to the boost converter and at which load values maximum power point (MPP) will follow. In another study, Benhadouga et al. (2022) performed MPPT with a boost converter using the sliding mode technique. They started their load from the lowest value and increased it up to about 50 Ω. They obtained the best MPP value around 5 Ω. Again, these researchers did not emphasize which loads are suitable for the boost converter.

Although many studies have been done using some converters, the relationship between selected load resistors, converter and input impedance has not been mentioned. Unlike other studies, in this study, a simulation of load behavior based on perturb-observation (P&O) method in non-isolated boost converter for maximum power point tracking of thermoelectric generators has been carried out by means of a TEG setup in MATLAB/Simulink.

2. MATERIAL AND METHOD

2.1. Principle of Maximum Power Point

The circuit diagram of TEG and load connection is given in Figure 1. The load resistance in the circuit varies continuously. The load in the TEG system is connected to obtain power from the TEG. MPP is reached when the load resistance and TEG internal resistance are equal (Bhuiyan et al., 2022). This situation cannot always be achieved because the load is not always the same and the overall resistance of the TEG varies depending on the temperature difference (Mamur and Çoban, 2020a). But this equality is always desired.

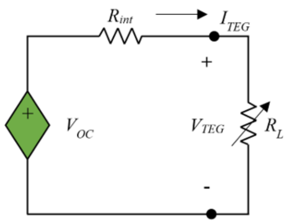

Figure 1. TEG load connection

The derivative of the power from TEG when MPP is zero:

$$\frac{dP}{dV_{TEG}}\,|_{max} = \frac{V_{OC}-2V_{TEG}}{R_{int}} = 0 \qquad (1)$$

Where, V_{OC} is the open circuit voltage of TEG in (V), V_{TEG} is the voltage obtained from TEG in (V), and R_{int} represents the internal resistance of TEG in (Ω) (Montecucco et al., 2014). The value of $V_{TEG/MAX}$ in MPP is half of the value of V_{OC} and is given by the below equation (Armin Razmjoo et al., 2020).

$$V_{TEG/MAX} = \frac{V_{OC}}{2} \qquad (2)$$

The maximum power from the TEG is explained by the following equation, depending on the open circuit voltage and internal resistance of the TEG:

$$P_{TEG\_MAX} = \frac{V_{OC}^2}{4R_{int}} \qquad (3)$$

Where, P_{TEG_MAX} is the maximum power of TEG in (W). TEG current and TEG voltage vary linearly depending on the load. MPP can also be extracted from the half of short-circuit current or open-circuit voltage of the TEG. Hence, the MPP voltage and MPP current are formulated by the given equation (Mamur and Üstüner, 2021):

$$V_{MPP} = V_{TEG/MAX} = \frac{V_{OC}}{2} \text{ or } I_{MPP} = I_{TEG/MAX} = \frac{I_{SC}}{2} \qquad (4)$$

Where, V_{MPP} is TEG MPP voltage in (V), I_{MPP} is the MPP current of the TEG in (A), and I_{SC} is the short-circuit current of the TEG in (A). When the load is directly linked to the end pins of the TEG, the efficiency of the TEG is further reduced if the internal resistance of the linked load and the TEG are not equal. This is called impedance imbalance. For minimizing the problem, DC-DC converters that carried out both maximum power point tracker (MPPT) and power arrangement are employed with TEGs. At that rate, the load of TEG becomes DC-DC converter (Bijukumar et al., 2019). Since the DC-DC converter linked between the TEG and the load is the load of the TEG, making the TEG overall internal resistance and the DC-DC converter resistance equal is carried out by the MPPT program. Thus, both the highest efficiency from TEG is obtained and voltage regulation is ensured (Tsai and Lin, 2010). Figure 2 illustrates the MPPT principle.

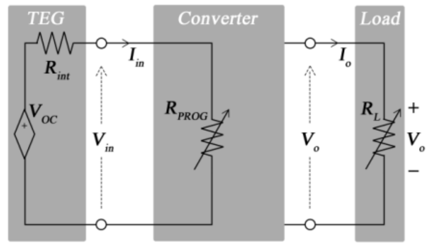

Figure 2. MPPT principle

When the converter is connected between TEG-load, now the load resistance of TEG is this DC-DC converter. This is expressed by R_{PROG} (Mamur et al., 2022).

2.2. Boost converter

A DC-DC converter is a circuit that converts DC voltage from one value to a higher value and operates with electronic switching. (Mamur and Çoban 2020b). As seen in Figure 3a, it consists of a coil, a switch, and a diode. Boost converters can be studied in 2 modes, Mode1 and Mode2, as seen in Figures 3b and 3c.

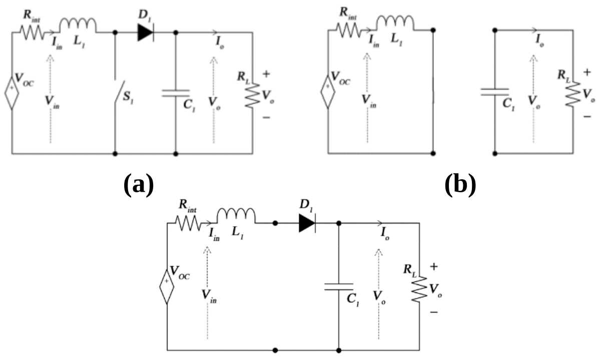

Figure 3. Boost converter **(a)** scheme, **(b)** Mode1, and **(c)** Mode2

In mode1, when the switch is on, the current comes from the source and flows through the coil and the switching element. In this way, energy is stored on the coil. In Mode2, when the switch is in off, the current circuit is completed via the diode and capacitor, not through the switching element. When the switch is conducting, the coil transfers the energy stored on the capacitor and the load via the diode. On the other hand, the capacitor charges when the switch is off, and discharges when the switch is on. When the switching process is fulfilled very fast, the coil is not completely discharged during charging and discharging and is always loaded. In this way, the energy of the source and coil is loaded into the capacitor (Taghvaee et al., 2013). The load is fed from the capacitor when the switch is in the conduction position, and from the source and coil when it is cut. Thus, a low DC voltage is converted to a higher DC voltage.

The transformation equation of a typical boost converter is given below:

$$\frac{V_o}{V_{in}} = \frac{1}{1-D} \tag{5}$$

$$V_{in} = V_o \times (1-D) \tag{6}$$

$$I_{in} = \frac{I_o}{1-D} \tag{7}$$

Where, V_o, V_{in}, D, I_{in}, and I_o are the output voltage in (V), the input voltage in (V), the duty cycle, the input current in (A) and the output current in (A) of the converter, respectively. The value of R_{PROG} in Figure 2 is the internal resistance of the inverter. Using the boost converter equations, the following result is obtained:

$$R_{PROG} = \frac{V_{in}}{I_{in}} = \frac{V_o \times (1-D)}{I_o/(1-D)} = \frac{V_o \times (1-D)^2}{I_o} = R_L \times (1-D)^2 \tag{8}$$

Where, R_L is the load resistance in (Ω). (8) shows that in boost converters, the resistance of load can be increased up to an infinite resistance non depending on the TEG internal resistance.

While calculating the boost converter, the D value is given by the following equation:

$$D = 1 - \frac{V_{in(\min)} \times \eta}{V_o} \tag{9}$$

Where, $V_{in(\min)}$ is the minimum input voltage of the converter in (V), and η is the efficiency of the converter. The ripple current of the coil is shown in the following equation:

$$\Delta I_L = \frac{V_{in(\min)} \times D}{f_S \times L} \tag{10}$$

Where, ΔI_L is the ripple current of the coil in (A), f_S is the switching frequency in (Hz), and L is the inductance of the coil in (H). Hence, the output current of the converter is given as below:

$$I_o = \frac{D \times (1-D) \times V_{in}}{2 \times L \times f_S} + (1-D) \times I_{min} \tag{11}$$

The maximum allowable output current of the converter can be calculated by two different equations. These are given below:

$$I_{o(max)} = \left(I_{LIM(min)} - \frac{\Delta I_L}{2}\right) \times (1-D) \tag{12}$$

$$I_{o(max)} = \sqrt{P_{TEG\_MAX}/R_L} \tag{13}$$

Where, $I_{o(max)}$ and $I_{LIM(min)}$ are the maximum allowable output current in (A), minimum allowable switching current in (A) of the converter, respectively. On the other hand, the maximum allowable output voltage of the converter is given below:

$$V_{o(max)} = \sqrt{P_{TEG\_MAX} \times R_L} \tag{14}$$

Where, $V_{o(max)}$ is the maximum output voltage value of the converter in (V). Along with these, the maximum switching current is given by the following equation:

$$I_{SW(max)} = \frac{\Delta I_L}{2} + \frac{I_{o(max)}}{1-D} \tag{15}$$

Where, $I_{o(max)}$, and $I_{LIM(min)}$ are the maximum allowable output current (A), minimum allowable switching current (A) of the converter, respectively. $I_{SW(max)}$ is the maximum switching current. The coil inductance equation of the converter is given below:

$$L = \frac{V_{in} \times (V_o - V_{in})}{\Delta I_L \times f_S \times V_o} \tag{16}$$

Since the coil value is not known in (10), the value of ΔI_L cannot be calculated. Therefore, the following equation is used:

$$\Delta I_L = (0.2 \sim 0.4) \times I_{o(max)} \times \frac{V_o}{V_{in}} \tag{17}$$

ΔI_L value fluctuates between 20% and 40% of the output current and is taken between these values. On the other hand, the required minimum capacitor value to be used in the boost converter is found with the following equation:

$$C_{out(min)} = \frac{I_{o(max)} \times (1-D)}{f_S \times \Delta V_o} \tag{18}$$

Where, $C_{out(min)}$ is the output capacitor (F). The output ripple voltage of the boost converter is given below:

$$\Delta V_o = ESR \times \frac{I_{o(max)}}{1-D} + \frac{\Delta I_L}{2} \tag{19}$$

Here, ΔV_o, and ESR are the output ripple voltage in (V) and the equivalent series resistance in (Ω) of the output capacitor used, respectively. The values calculated according to the equations used are shown in Table 1.

Table 1. The boost converter calculated values

Parameter	Value	Unit	Description
P_{TEG_MAX}	45.76	W	Power at MPP
P_{conv}	50	W	Power of converter
V_{in}	16.4	V	Input voltage
R_L	1-45	Ω	Load resistance
$I_{o(max)}$	$\sqrt{P_{TEG\_MAX}/R_L}$	A	Max output current
$V_{o(max)}$	$\sqrt{P_{TEG\_MAX} \times R_L}$	V	Max output voltage
ΔI_L	30% of I_o	A	Max ripple current
ΔV_o	5% of V_o	A	Max voltage ripple
η	0.8		Converter efficiency
f_s	20	kHz	Frequency
L_1	~62	µH	Inductance
C_1	~2400	µF	Capacitance

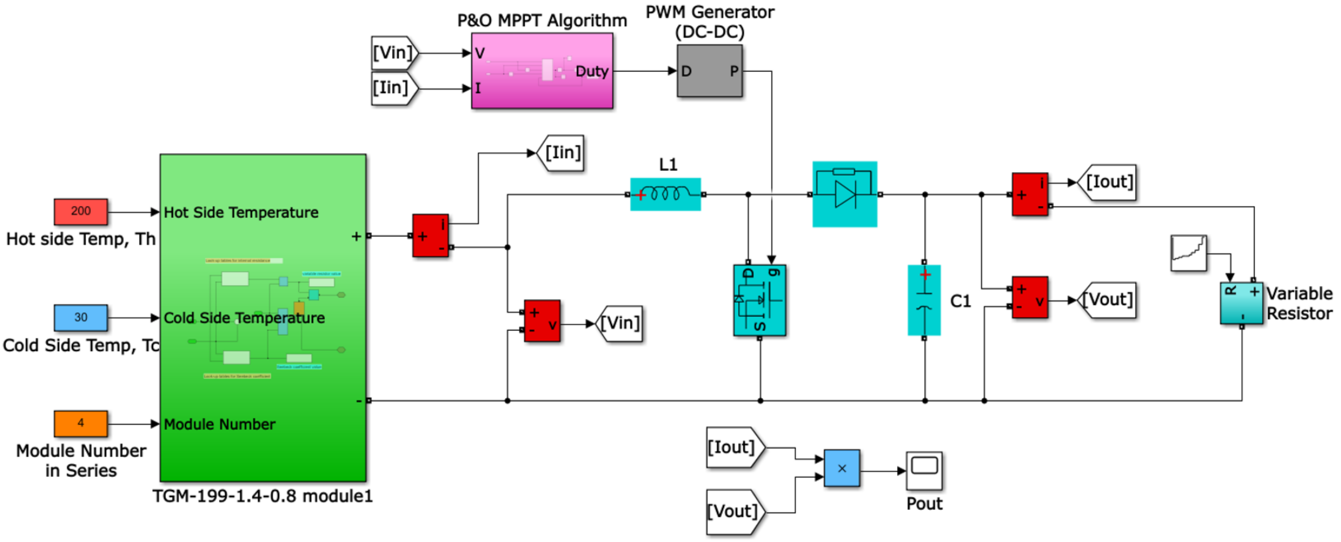

Figure 5. TEG system-converter and load connection

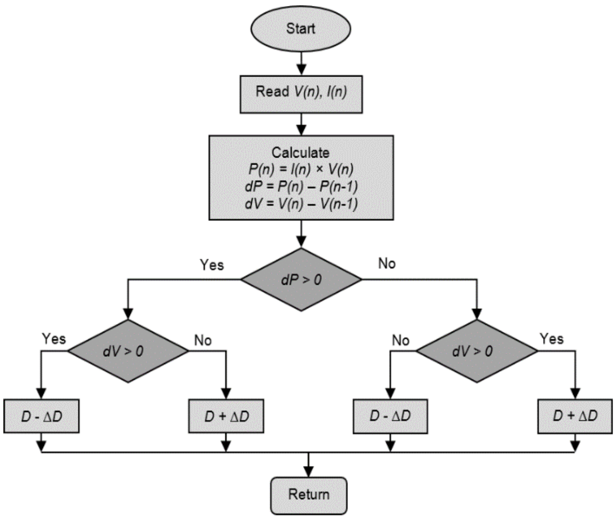

Figure 4. P&O MPPT algorithm

2.3. Perturb and observe algorithm

The most popular of MPPT methods is the P&O algorithm (Qasim et al., 2021), whose flow diagram is given in Figure 4. MPPT is required because when a power is generated from TEGs, the change in load and the change in temperature causes a difference in the generated MPP value. Power conditioning methods are used to capture MPP in TEGs. One of the power conditioning methods is impedance matching. The P&O MPPT algorithm fulfils the impedance matching. The algorithm adjusts the duty cycle of the switch in the converter operated in the setup. First, current and voltage values are obtained by means of current sensor and voltage sensor. Using the measured current and voltage value, the power, the changes of power, and of voltage are calculated. Then, the power change is questioned (Pilakkat et al., 2019). If the power change is positive, the voltage change is questioned. If this is also positive, the D value is lowered by ΔD. Here, if the voltage change is negative, the D value is raised by ΔD. It's back to the beginning. By making a new measurement, the power value is figured out, and new power and voltage changes are found. According to these found values, if the power change is negative, the voltage change is again questioned. If the voltage change is positive, the D value is increased by ΔD. If the voltage change is negative, the D value is reduced by ΔD. The process is continued until the MPP value (Sarbu and Sebarchievici, 2018).

Although this P&O algorithm has a disadvantage MPP, oscillations occur around the MPP as the process is still running. Large ΔD ranges result in rapid MPP capture, resulting in ample oscillations in MPP (Al-Diab et all., 2010). On the other hand, small ΔD intervals result in slow MPP capture while reducing the magnitude of MPP oscillations. Another drawback is that when the temperature difference changes, the MPP will change and in this case a separate oscillation will occur to find the new MPP (Jouhara et al., 2018).

2.4. TEG setup

A TEG setup was designed in the MATLAB/Simulink software to carry out the study. In this TEG system, as many TEG modules as desired can be linked in series and parallel. The amount of power obtained varies according to the serial and parallel connection. A boost converter has been added to the TEG system, whose design calculations have been made. A gradually adjusted load is connected to the end pins of the boost converter. Figure 5 shows this TEG system-converter and load connection.

The internal resistance values of these TEG modules change depending on the temperature. Desired temperature ranges can be given with input values. The P&O MPPT method is operated to switch the boost converter. In the simulation study, the power obtained from the TEG to the converter and the power given by the converter to the load resistor were measured. The overall internal resistance of the TEG system is 5.84 Ω. The load resistors linked the converter were gradually changed to 1, 3, 5.84, 7, 9, 11, 15, 20, 30 and 45 Ω.

The hot surface temperature of the TEG setup was hold steady at $T_H = 200°C,$ and the cold surface temperature at$T_C = 30°C$. Then, the variation of the output power obtained according to the changing loads was observed. The duty cycle D values produced by means of the P&O MPPT method depending on the variability of the load have been changed (Mamur et al, 2022).

3. RESULTS

In the simulation study performed in MATLAB/Simulink software, the load values of the TEG system were changed gradually. It would be better to think of these modified values as values above and below the overall internal resistance of the TEG system. In the study carried out, these values below 5.84 Ω are these values below the overall internal resistance of the TEG system. These values 5.84 Ω and above are these values above the overall internal resistance of the TEG system. In addition, analysis was made for the case of $R_{int} = R_L$, where it is equal. The MPP value of the modeled TEG system is 45.76 W.

The D value produced by the P&O MPPT algorithm has to be zero according to equation (8) to obtain the maximum load value at load resistance values below 5.84 Ω. In simulation studies, the minimum D value was determined as 0.05 to prevent the converter from turning off or to keep it on continuously, as given in Table 2. In cases where the resistance of load is less than the overall internal resistance, the boost converter switch is expected to operate with a minimum value of D. When the value of the resistor of load is increased, it is hoped that the P&O MPPT algorithm will keep the $R_{int} = R_L$ state continuously by increasing the D value of the boost converter switch, so that the system will remain at the MPP value, since the overall internal resistance of the TEG setup is equal to the resistance of load.

The curves of change in current, voltage, and power in the TEG system under constant surface temperatures and variable loads of the TEG, performed in the MATLAB/Simulink simulation software, are illustrated in Figure 6. Depending on these load changes, the change in the D value of the boost converter switch generated by means of the P&O MPPT algorithm to catch the MPP value is given in Figure 7. In addition, the average D values produced according to the load changes are presented in Table 2. It would be appropriate to evaluate this Figure 6 and Figure 7 together.

There are two cases where the resistance of load is less than the overall internal resistance in the TEG setup. These are 1 Ω and 3 Ω values. The D value in these two cases was 0.05. For impedance matching, the system worked with a minimum D value. In these two cases, they are 19.88 W and 37.42 W, respectively, as given in Table 2.

In the third case, the $R_{int} = R_L$ condition is desirable. The P&O MPPT algorithm produced an average of 0.06 D, keeping the impedance matching state and reaching the MPP value with 43.4 W. When the resistance of load was changed to 7 Ω, 9 Ω, 11 Ω and 15 Ω, the P&O MPPT algorithm was able to perform impedance matching, producing D values of 0.097, 0.199, 0.27 and 0.348, respectively. The MPP values obtained from the TEG system in these cases were 43.38 W, 42.76 W, 42.11 W and 40.93 W, respectively.

When the value of the load resistance in the stepped TEG system applied in MATLAB/Simulink environment is changed to 20 Ω, 30 Ω and 45 Ω, the obtained power values are 39.55 W, 37.32 W and 34.53 W, respectively. D values produced depending on these load values are 0.414, 0.496 and 0.547, respectively.

4. DISCUSSION AND CONCLUSIONS

In this study, which was carried out in MATLAB/Simulink environment, a 50 W converter was designed for the TEG system with a maximum power of 45.76 W and a converter with P&O MPPT was used to prevent it from being affected by different loads. The boost converter was operated with the D values produced by the P&O MPPT algorithm according to the connected load values.

At the resistance values of load lower than the internal resistance of the TEG system, MPP cannot be followed due to the working principle of the boost converter. In the study, this situation is clearly seen in the first two resistance values of the MATLAB/Simulink simulation studies. In cases where the load resistance values connected with the overall internal resistance of the TEG system are equal and large, the boost converter working with the D values generated by means of the P&O MPPT algorithm provides the MPP value by matching the impedance. However, approaching the full MPP value is difficult due to the losses in the boost converter. However, at high load values, the power value that drops considerably without utilizing a boost converter embedded MPPT enables the follow-up of MPP when utilizing a boost converter embedded P&O MPPT algorithm. However, when high load values are reached, the output voltage of the boost converter increases with increasing D values and the MPPT error percentage increases. In R_L of 5,84 Ω, D, P_{MPP} and error values are 0.06 and 43.4 W and 5.16, respectively.

As a result, in this study, a boost converter embedded P&O MPPT algorithm by a program software is linked between TEG and load to reach the power obtained from TEG to MPP value. The task of this boost converter is to ensure that the power obtained from the TEG is not affected by load changes. The load resistance value of the boost converter with P&O MPPT algorithm does not function from the minimum to the internal resistance value of the TEG. However, when the TEG reaches its overall internal resistance and rises above this value, the P&O MPPT algorithm starts to function. While the best MPP tracking is close to the internal resistance value, MPP tracking is performed at the load resistance values above it. However, as the load resistance increases, the MPPT error increases. As a result, MPP monitoring can be made between the TEG overall internal resistance and the infinite load resistance with the boost converter with P&O MPPT. The most efficient MPPT can be made up to about three times the internal resistance of the TEG.

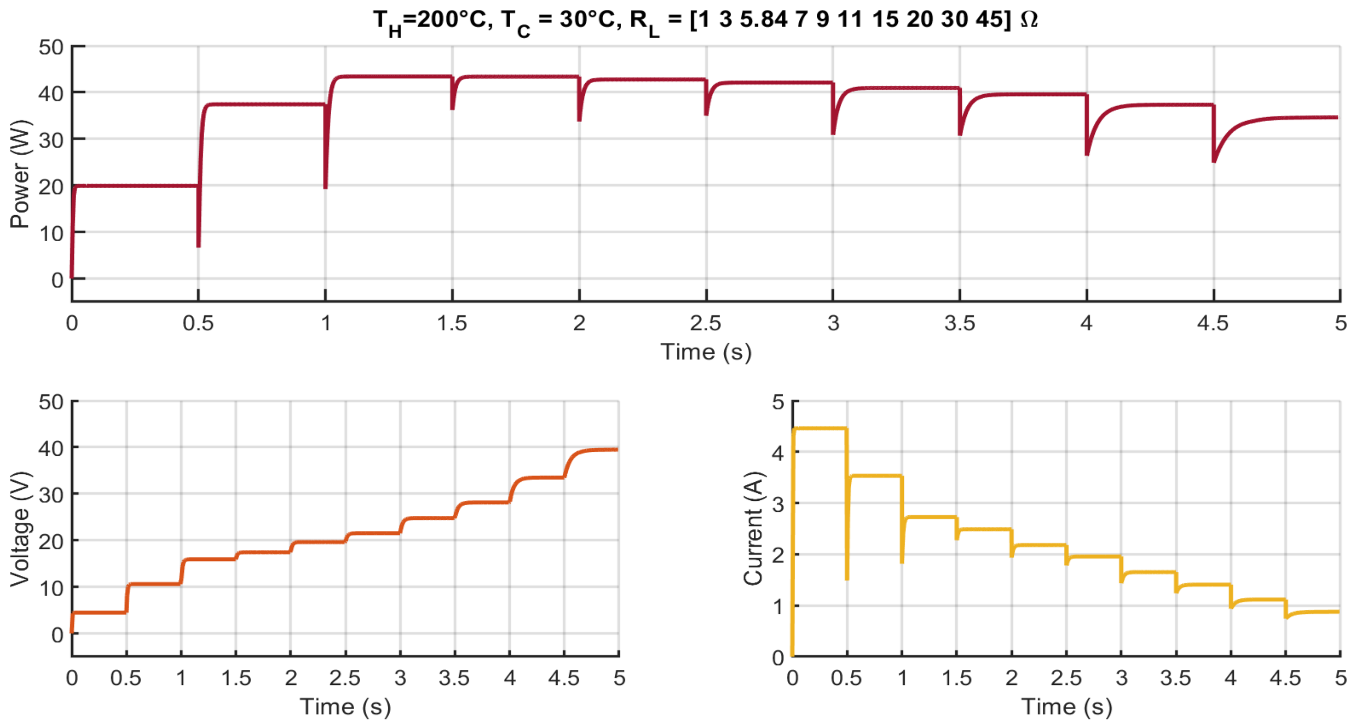

Figure 6. The curves in power, voltage and current of TEG system under variable loads

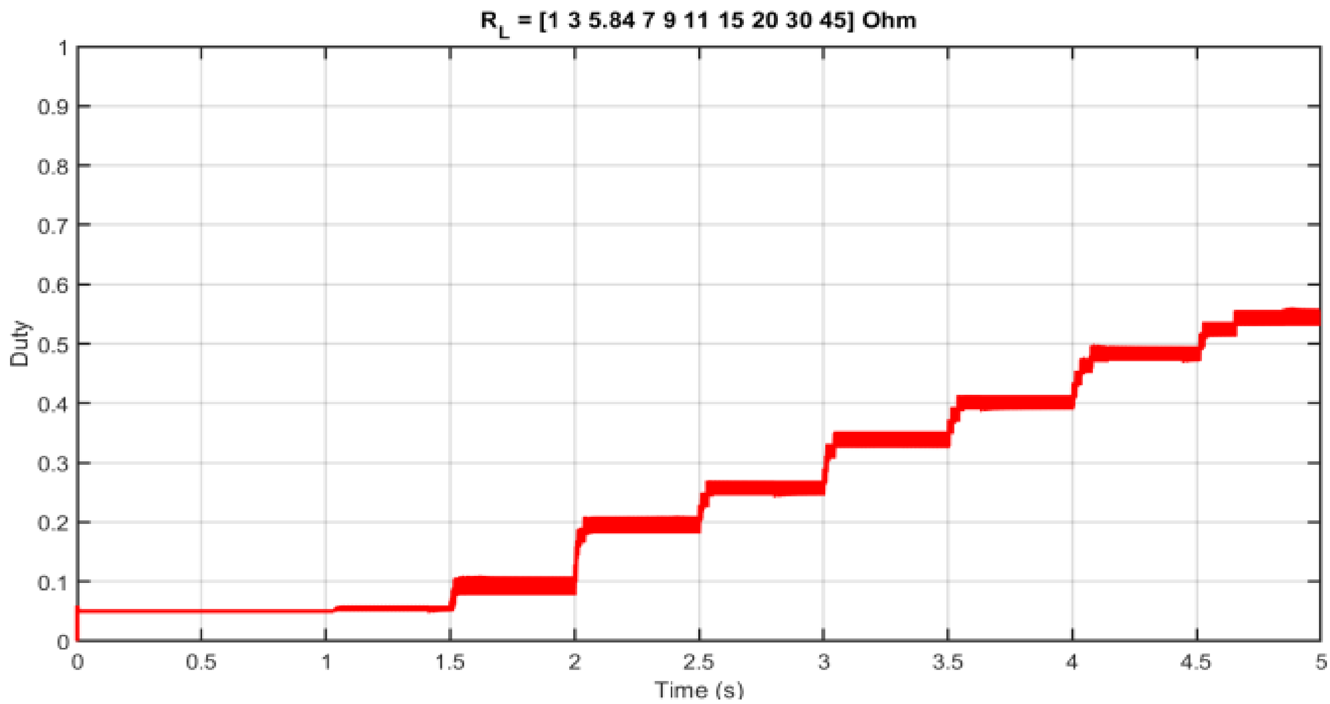

Figure 7. Duty cycle rate under variable loads

Table 2. Average *D* values produced according to load changes.

	R_L values (Ω)									
	1	3	5.84	7	9	11	15	20	30	45
D	0.05	0.05	0.06	0.097	0.199	0.27	0.348	0.414	0.496	0.547
P_{MPP}(W)	19.88	37.42	43.4	43.38	42.76	42.11	40.93	39.55	37.32	34.53
Error (%)	56.56	18.23	5.16	5.20	6.56	7.98	10.56	13.57	18.44	24.54

Acknowledgements
This work was supported by Research Project Coordination Unit of The Manisa Celal Bayar University (Project Number 2022-027). In addition, this study was published in full text at the International Conference on Science and Technology (ICONST 2022, 7-9 September, Budva, Montenegro).

Ethics Committee Approval
N/A

Peer-review
Externally peer-reviewed.

Author Contributions
Conceptualization: H.M., Investigation: Ç.A., M.A.Ü.; Material and Methodology: H.M., Ç.A., M.A.Ü.; Supervision: H.M., Visualization: Ç.A., M.A.Ü.; Writing-Original Draft: Ç.A., M.A.Ü.; Writing-review & Editing: H.M., Ç.A., M.A.Ü.; Other: All authors have read and agreed to the published version of manuscript.

Conflict of Interest
The authors have no conflicts of interest to declare.

REFERENCES

Ahmad, M. E., Numan, A. H., Mahmood, D. Y. (2022). A comparative study of perturb and observe (P&O) and incremental conductance (INC) PV MPPT techniques at different radiation and temperature conditions. Engineering and Technology Journal, 40(02), 376-385. http://doi.org/10.30684/etj.v40i2.2189

Al-Diab, A., Sourkounis, C. (2010, May). Variable step size P&O MPPT algorithm for PV systems. In 2010 12th International conference on optimization of electrical and electronic equipment (pp. 1097-1102). IEEE. http://doi.org/10.1109/OPTIM.2010.5510441

Armin Razmjoo, A., Sumper, A., Davarpanah, A. (2020). Energy sustainability analysis based on SDGs for developing countries. Energy Sources, Part A: Recovery, Utilization, and Environmental Effects, 42(9), 1041-1056. http://doi.org/10.1080/15567036.2019.1602215

Attar, A., Lee, H., Snyder, G. J. (2020). Optimum load resistance for a thermoelectric generator system. Energy Conversion and Management, 226, 113490. http://doi.org/10.1016/j.enconman.2020.113490

Benhadouga, S., Meddad, M., Eddiai, A., Boukhetala, D., Khenfer, R. (2019). Sliding Mode Control for MPPT of a Thermogenerator. Journal of Electronic Materials, 48, 2103-2111. https://doi.org/10.1007/s11664-019-06997-y

Bijukumar, B., Raam, A. G. K., Ganesan, S. I., Nagamani, C., Reddy, M. J. B. (2019). MPPT algorithm for thermoelectric generators based on parabolic extrapolation. IET Generation, Transmission & Distribution, 13(6), 821-828. http://doi.org/10.1049/iet-gtd.2017.2007

Bhuiyan, M. R. A., Mamur, H., Üstüner, M. A., Dilmaç, Ö. F., (2022). Current and future trend opportunities of thermoelectric generator applications in waste heat recovery. Gazi University Journal of Science, 896-915. http://doi.org/10.35378/gujs.934901

Bond, M., Park, J. D. (2015). Current-sensorless power estimation and MPPT implementation for thermoelectric generators. IEEE Transactions on Industrial Electronics, 62(9), 5539-5548. http://doi.org/10.1109/TIE.2015.2414393

Dileep, G., Singh, S. N. (2017). Selection of non-isolated DC-DC converters for solar photovoltaic system. Renewable and Sustainable Energy Reviews, 76, 1230-1247. http://doi.org/10.1016/j.rser.2017.03.130

Jouhara, H., Khordehgah, N., Almahmoud, S., Delpech, B., Chauhan, A., Tassou, S. A. (2018). Waste heat recovery technologies and applications. Thermal Science and Engineering Progress, 6, 268-289. http://doi.org/10.1016/j.tsep.2018.04.017

Khan, M. K., Zafar, M. H., Mansoor, M., Mirza, A. F., Khan, U. A., & Khan, N. M. (2022). Green energy extraction for sustainable development: A novel MPPT technique for hybrid PV-TEG system. Sustainable Energy Technologies and Assessments, 53, 102388. https://doi.org/10.1016/j.seta.2022.102388

Mamur, H., Ahiska, R. (2015). Application of a DC–DC boost converter with maximum power point tracking for low power thermoelectric generators. Energy conversion and management, 97, 265-272. http://doi.org/10.1016/j.enconman.2015.03.068

Mamur, H., Coban, Y. (2020a). Detailed modeling of a thermoelectric generator for maximum power point tracking. Turkish Journal of Electrical Engineering & Computer Sciences, 28(1), 124-139. http://doi.org/10.3906/elk-1907-166

Mamur, H., Çoban, Y. (2020b). Termoelektrik jeneratörler için alçaltan-yükselten çeviricili maksimum güç noktası takibi benzetimi. Pamukkale Üniversitesi Mühendislik Bilimleri Dergisi, 26(5), 916-926. http://doi.org/10.5505/pajes.2019.92488

Mamur, H., Dilmaç, Ö. F., Begum, J., Bhuiyan, M. R. A. (2021). Thermoelectric generators act as renewable energy sources. Cleaner Materials, 2, 100030.

Mamur, H., Üstüner, M. A. (2021) Improved perturb and observe maxımum power poınt trackıng method wıth thermoelectrıc generator model. International Scientific Conferance, Gabrova.

Mamur, H., Üstüner, M. A., Bhuiyan, M. R. A., (2022). Future perspective and current situation of maximum power point tracking methods in thermoelectric generators. Sustainable Energy Technologies and Assessments, 50, 101824. http://doi.org/10.1016/j.clema.2021.100030

Montecucco, A., Knox, A. R. (2014). Maximum power point tracking converter based on the open-circuit voltage method for thermoelectric generators. IEEE Transactions on Power Electronics, 30(2), 828-839. http://doi.org/10.1109/TPEL.2014.2313294

Pilakkat, D., Kanthalakshmi, S. (2019). An improved P&O algorithm integrated with artificial bee colony for photovoltaic systems under partial shading conditions. Solar Energy, 178, 37-47.

http://doi.org/10.1016/j.solener.2018.12.008

Sarbu, I., Sebarchievici, C. (2018). A comprehensive review of thermal energy storage. Sustainability, 10(1), 191. http://doi.org/10.3390/su10010191

Taghvaee, M. H., Radzi, M. A. M., Moosavain, S. M., Hizam, H., Marhaban, M. H., (2013). A current and future study on non-isolated DC–DC converters for photovoltaic applications. Renewable and Sustainable Energy Reviews, 17, 216-227. http://doi.org/10.1016/j.rser.2012.09.023

Tsai, H. L., Lin, J. M. (2010). Model building and simulation of thermoelectric module using Matlab/Simulink. Journal of Electronic Materials, 39(9), 2105. http://doi.org/10.1007/s11664-009-0994-x

Qasim, A. M., Alwan, T. N., PraveenKumar, S., Velkin, V. I., Agyekum, E. B. (2021). A New maximum power point tracking technique for thermoelectric generator modules. Inventions, 6(4), 88. http://doi.org/10.3390/inventions6040088

Mamur, H., Çiğdem, A., Üstüner, M.A. (2022, Sep). Investigation of Load Dependent Behavior of Boost Converter with Perturb and Observe Maximum Power Point Tracking for Thermoelectric Generators, In International Conferences on Science and Technology Engineering Sciences and Technology (ICONST EST 2022).

Zafar, M. H., Khan, N. M., Mansoor, M., & Khan, U. A. (2022). Towards green energy for sustainable development: Machine learning based MPPT approach for thermoelectric generator. Journal of Cleaner Production, 351, 131591. https://doi.org/10.1016/j.jclepro.2022.131591